

# Involvement of P2X<sub>7</sub> receptors in the regulation of neurotransmitter release in the rat hippocampus

Beáta Sperlágh,\* Attila Köfalvi,\* Jim Deuchars,† Lucy Atkinson,† Carol J. Milligan,† Noel J. Buckley†‡ and E. Sylvester Vizi\*

\*Institute of Experimental Medicine, Hungarian Academy of Sciences, Budapest, Hungary

†School of Biomedical Sciences and ‡Department of Biochemistry and Molecular Biology, University of Leeds, Leeds, UK

## Abstract

Although originally cloned from rat brain, the P2X<sub>7</sub> receptor has only recently been localized in neurones, and functional responses mediated by these neuronal P2X<sub>7</sub> receptors (P2X<sub>7</sub>R) are largely unknown. Here we studied the effect of P2X<sub>7</sub>R activation on the release of neurotransmitters from superfused rat hippocampal slices. ATP (1–30 mM) and other ATP analogues elicited concentration-dependent [<sup>3</sup>H]GABA outflow, with the following rank order of potency: benzoylbenzoylATP (BzATP) > ATP > ADP. PPADS, the non-selective P2-receptor antagonist (3–30 μM), Brilliant blue G (1–100 nM) the P2X<sub>7</sub>-selective antagonist and Zn<sup>2+</sup> (0.1–30 μM) inhibited, whereas lack of Mg<sup>2+</sup> potentiated the response by ATP. *In situ* hybridization revealed that P2X<sub>7</sub>R mRNA is expressed in the neurones of the cell body layers in the hippocampus. P2X<sub>7</sub>R immunoreactivity was found in excitatory synaptic terminals in CA1 and CA3 region targeting

the dendrites of pyramidal cells and parvalbumin labelled structures. ATP (3–30 μM) and BzATP (0.6–6 μM) elicited concentration-dependent [<sup>14</sup>C]glutamate efflux, and blockade of the kainate receptor-mediated transmission by CNQX (10–100 μM) and gadolinium (100 μM), decreased ATP evoked [<sup>3</sup>H]GABA efflux. The Na<sup>+</sup> channel blocker TTX (1 μM), low temperature (12°C), and the GABA uptake blocker nipecotinic acid (1 mM) prevented ATP-induced [<sup>3</sup>H]GABA efflux. Brilliant blue G and PPADS also reduced electrical field stimulation-induced [<sup>3</sup>H]GABA efflux. In conclusion, P2X<sub>7</sub>Rs are localized to the excitatory terminals in the hippocampus, and their activation regulates the release of glutamate and GABA from themselves and from their target cells.

**Keywords:** ATP, GABA, hippocampus, immunocytochemistry, P2X receptors, release.

*J. Neurochem.* (2002) **81**, 1196–1211.

P2X receptors are ligand-gated ion channels, conveying the action of extracellular ATP and other nucleotides. Seven different P2X receptor subunits have been identified which can form as many as 17 different homo- or heterooligomeric combinations (Torres *et al.* 1999). Although the exact composition of native P2X receptors is still largely unknown, it is apparent that they are pharmacologically diverse, suggesting different heteromultimeric assemblies underlie this disparity (Khakh 2001).

ATP is co-stored and co-released with classical neurotransmitters from central neurones (Sperlágh and Vizi 1996; Sperlágh and Vizi 2000) and – activating P2X receptor subtypes – acts as a fast neurotransmitter in the brain (Edwards *et al.* 1992; Norenberg and Illes 2000; Khakh 2001). In addition, ATP can directly initiate neurotransmitter release by the activation of presynaptic P2X receptors, e.g. those located on axon terminals of autonomic and sensory nerves (Sperlágh and Vizi 1991; Gu and MacDermott 1997;

Received October 23, 2001; accepted February 25, 2002.

Address correspondence and reprint requests to Beáta Sperlágh, Department of Pharmacology, Institute of Experimental Medicine, Hungarian Academy of Sciences, H-1450 Budapest, POB 67, Hungary. E-mail: sperlagh@koki.hu

**Abbreviations used:** AMPA, α-amino-3-hydroxy-5-methylisoxazole-4-propionic acid; AP-5, D(-)-2-amino-5-phosphonopentanoic acid; AUC, area under the curve; BzATP, 2'- & 3'-O-(4-benzoyl-benzoyl)adenosine 5'-triphosphate; CNQX, 6-cyano-7-nitroquinoxaline-2,3-dione-disodium; DAB, diaminobenzidine; DDW, distilled deionized water; DG, dentate gyrus; DHβE, dihydro-β-erythroidine hydrobromide; DMPX, 3,7-dimethyl-1-propargylxanthine; EAA, excitatory amino acid; EFS, electrical field stimulation; EM, electron microscopy; Gd<sup>3+</sup>, gadolinium; HPLC, high-performance liquid chromatography; mRNA, messenger RNA; NF279, 8,8'-(Carbonylbis(imino-4,1-phenylenecarbonylimino-4,1-phenylenecarbonylimino))bis (1,3,5-naphthalenetrisulfonic acid; oxoATP, adenosine 5'-triphosphate periodate oxidized; PB, phosphate buffer; PBS, phosphate-buffered saline; PPADS, pyridoxalphosphate-6-azophenyl-2',4'-disulfonic acid; P2X<sub>7</sub>R, P2X<sub>7</sub> receptor; TTX, tetrodotoxin; TNP-ATP, 2'-(or-3')-O-(2,4,6-trinitrophenyl)adenosine 5'-triphosphate trisodium.

Hugel and Schlichter 2000; Sperlagh *et al.* 2000). P2X receptors, furthermore, are expressed also on non-neuronal cells and are involved in a variety of functions including neuron–glia interactions, host defense reaction and immunomodulation (Burnstock 1999; Illes *et al.* 2000).

Amongst the P2X receptors, P2X<sub>7</sub> receptors (P2X<sub>7</sub>R) are unique because in expression systems they function only in homooligomeric form and bear a pharmacological profile markedly different from other P2X homo- or heteromers (North and Surprenant 2000). This subtype was cloned for the first time from brain tissue (Surprenant *et al.* 1996), where it was suggested to be localized to activated microglia and therefore implicated with a role in immune responses. Such a role for the P2X<sub>7</sub> receptor is consistent with its involvement in the inflammatory process, e.g. in cytokine and nitric oxide production, cytotoxicity and cell proliferation (Di Virgilio *et al.* 1999) and localization to cells of the immune system such as the monocyte-macrophages and microglia (Collo *et al.* 1997). Nevertheless, recently it has been reported that P2X<sub>7</sub>R is expressed in the rat retinal and cochlear ganglion cells (Brandle *et al.* 1998, 1999) and P2X<sub>7</sub>R immunoreactivity is present on excitatory nerve terminals in the brain stem and the spinal cord (Deuchars *et al.* 2001), indicating that neuronal cells may also express this receptor.

In the hippocampus, ATP is released upon high frequency electrical field stimulation (Cunha *et al.* 1996) and direct stimulation of Schaffer collaterals (Wieraszko *et al.* 1989) and it acts as a fast transmitter via activation of postsynaptic P2X receptors (Pankratov *et al.* 1998; Mori *et al.* 2001). Such postsynaptic P2X receptors have been reported by immunohistochemical localization of P2X<sub>2</sub>, P2X<sub>4</sub> and P2X<sub>6</sub> receptor subunits at excitatory postsynaptic specializations in the CA1 region of the hippocampus (Rubio and Soto 2001). However, there is no direct functional or anatomical evidence of presynaptically located P2X receptors in the hippocampus.

Therefore to study presynaptic function we assessed the effect of ATP and its analogues on neurotransmitter efflux from superfused hippocampal slices. We demonstrate that activation of P2X<sub>7</sub>Rs in the hippocampus has a profound effect on the release of GABA and glutamate. In addition, we show neuronal expression of mRNA encoding P2X<sub>7</sub> receptors and immunohistochemical localization to the excitatory nerve terminals in the hippocampus, the activation of which could control the release of glutamate and subsequent GABA release.

## Materials and methods

All studies were conducted in accordance with the principles and procedures outlined in the NIH Guide for the Care and use of Laboratory animals and were approved by the local Animal Care Committee of the Institute of Experimental Medicine (Hungary), or

under a UK Home Office License in accordance with the regulations of the UK Animals (Scientific Procedures) Act 1986.

### Neurotransmitter release experiments from rat hippocampal slices

[<sup>3</sup>H]GABA release experiments were carried out as previously described (Katona *et al.* 1999; Köfalvi *et al.* 2000). Male Wistar rats (140–160 g, breeder: Gedeon Richter Ltd, Budapest, Hungary) were decapitated under CO<sub>2</sub> anaesthesia and the brain was quickly put into ice-cold Krebs' solution (NaCl 115 mM, KCl 3 mM, KH<sub>2</sub>PO<sub>4</sub> 1.2 mM, MgSO<sub>4</sub> 1.2 mM, CaCl<sub>2</sub> 2.5 mM, NaHCO<sub>3</sub> 25 mM, glucose 10 mM, pH 7.4), oxygenated with 95% O<sub>2</sub>, and 5% CO<sub>2</sub>. Both hippocampi were rapidly dissected and 400-µm thick slices were cut transversely with a McIlwain tissue chopper and incubated in 1 mL oxygenated Krebs' solution containing 4 µCi 4-aminon-[2,3-<sup>3</sup>H]butyric acid ([<sup>3</sup>H]GABA, specific activity 86.0 Ci/mmol, Amersham Pharmacia Biotech UK, Buckinghamshire, UK) for 60 min at 37°C. The incubating solution was supplemented with β-alanine (1 mM) to prevent tritium uptake into glial cells (Iversen and Kelly 1975). After incubation, the slices were rinsed three times with 6 mL Krebs' solution, and each slice was transferred to one of four polypropylene tissue chambers, and were perfused continuously with 95% O<sub>2</sub>- and 5% CO<sub>2</sub>-saturated Krebs' solution (37°C, flow rate: 0.6 mL/min). To minimize the formation of GABA metabolites, the perfusion solution contained aminooxyacetic acid (100 µM). Upon termination of the 60 min preperfusion period, 3 min samples of the effluent were collected and assayed for [<sup>3</sup>H]GABA. Except when electrical field stimulation-induced [<sup>3</sup>H]GABA release was studied, AP-5 (10 µM) and CNQX (10 µM) were added to the perfusion solution in order to block NMDA- and AMPA-receptor-mediated excitatory synaptic transmission, in the last 10 min of preperfusion period and thereafter. In the sample collection period, three kinds of protocols were applied:

(i) When the effect of P2X agonists on the basal outflow of [<sup>3</sup>H]GABA was studied 1 min long perfusions of agonists of increasing concentration were applied consecutively 15 min apart. ATP (10 mM) shifted the pH of the Krebs' solution from 7.4 ± 0.01 to 7.00 ± 0.01 (*n* = 4), nevertheless a similar acidification of Krebs' solution by HCl resulted in only a small elevation of the basal tritium efflux (*S*<sub>pH</sub> = 0.008 ± 0.001%, *n* = 7, *p* > 0.05). ATP (30 mM) changed the pH of the Krebs' solution to 4.93 ± 0.03 (*n* = 4) which also elicited only a negligible change in [<sup>3</sup>H]GABA efflux (*S*<sub>pH</sub> = 0.014 ± 0.01%, *n* = 4, *p* > 0.05), indicating that the majority of ATP-evoked release is independent from the change of pH. In some experiments P2 antagonists [suramin (300 µM), PPADS (30 µM), NF 279 (2 µM), Reactive Blue 2 (20 µM), TNP-ATP (30 µM)], or Mg<sup>2+</sup>-free Krebs' solution, were applied 10 min before the beginning of the sample collection period. Perfusion of oxidized ATP (300 µM) began 2 h before the sample collection period.

(ii) In other experiments, two 1-min-long perfusions of agonist (ATP) were administered in the beginning of the collection of 3rd and 13th samples (*S*<sub>ATP1</sub> and *S*<sub>ATP2</sub>) with identical concentrations, and drugs (PPADS, Brilliant blue G, atropine, DhβE, DMPX, tetrodotoxin, AP-5, CNQX, calmidazolium, Gd<sup>3+</sup>, GYKI 53655 or Zn<sup>2+</sup>) were added in the perfusion solution or the bath was fast cooled to 12°C 15 min before *S*<sub>ATP2</sub> as described earlier (Vizi 1998; Vizi and Sperlagh 1999) by the Frigomix R thermoelectric device

(Braun Instruments, Darmstadt, Germany), and all procedures lasted till the end of the sample collection period.

(iii) In some experiments, electrical field-stimulation (EFS<sub>1</sub>, EFS<sub>2</sub>; 35 V, 10 Hz, 1 ms, 360 bipolar, square-wave pulses) was applied using a Grass S88 Stimulator (Grass Medical Instruments, Quincy, MA, USA) via a pair of platinum ring electrodes in every tissue chamber in the beginning of the collection of 3rd and 13th samples; drugs were applied into the perfusion solution 15 min before EFS<sub>2</sub> [tetrodotoxin (1 μM), Brilliant blue G (100 nM); PPADS (30 μM)] and thereafter or in other experiments the bath was fast cooled to 12°C 15 min before EFS<sub>1</sub>.

### Subregion preparation

Following the procedure described by Milusheva *et al.* (1994), slices were gently dissected into tissue parts containing mainly CA1, CA3 or dentate gyrus (DG) by the use of a binocular microscope. This procedure was performed in ice-cold Krebs' solution continuously gassed with 95% O<sub>2</sub> and 5% CO<sub>2</sub>. After that the slices were left at room temperature in bubbled Krebs solution for 60 min, then the experiment was continued as described above. In one tissue chamber approximately 10 mg tissue was placed dissected from 8 to 10 slices.

### [<sup>14</sup>C]glutamate assay

In some experiments, hippocampal slices were pre-loaded with [<sup>14</sup>C]glutamic acid (specific activity 270 mCi/mmol, Amersham), for 45 min instead of [<sup>3</sup>H]GABA. Slices were then rinsed, superfused with oxygenated Krebs' solution and stimulated as described above. However, to minimize the spontaneous firing of CA1 and CA3 pyramidal cells, the bath temperature in these experiments were kept at 32°C. In previous studies using similar protocols (Di Iorio *et al.* 1996), it was shown that [<sup>14</sup>C]glutamate is a good indicator of endogenous glutamate release.

### Radioactivity assay

The radioactivity released from the preparations was measured with a Packard 1900 Tricarb liquid scintillation spectrometer (Canberra, Australia), which is equipped with Dynamic Colour Corrected DPM Option providing absolute activity (DPM) calculation and correction for all kinds of colour quenching. In an effort to determine the contribution of [<sup>3</sup>H]GABA to the total tritium efflux, the composition of the samples collected under resting conditions and during the peak of EFS- and 10 mM ATP-evoked response were analysed by high-performance liquid chromatography (HPLC) with fluorometric detection as described earlier (Nakai *et al.* 1999), and the amount of [<sup>3</sup>H]GABA was expressed in percentage of the total tritium content as 100%. The majority of the tritium label in the tissue (94.5 ± 1.1%) and in the resting effluent (69.9 ± 3.5%) represented [<sup>3</sup>H]GABA; the rest of the effluent represented [<sup>3</sup>H]aspartate indicating a minor extent of extraneuronal GABA metabolism. The ratio of [<sup>3</sup>H]GABA in the total tritium label was significantly higher in the samples collected during the peak of ATP-evoked response (85.9 ± 2.0% *p* < 0.01), showing that ATP primarily released [<sup>3</sup>H]GABA.

The release of [<sup>3</sup>H]GABA or [<sup>14</sup>C]glutamate was calculated in percentage of the amount of radioactivity in the tissue at the sample collection time (fractional release, %). The tissue tritium uptake was determined as the sum release + the tissue content after the experiment. The release of [<sup>3</sup>H]GABA or [<sup>14</sup>C]glutamate evoked by

agonists (S<sub>ATP1</sub>, S<sub>ATP2</sub>) or electrical field stimulation (EFS<sub>1</sub>, EFS<sub>2</sub>) was calculated by the area under the curve (AUC) method, i.e. subtracting the resting release expected to be released, calculated from the pre- and post-stimulation period, from the release evoked by stimulation, which lasted until a sample tritium content was equal to the pre-stimulation period sample contents.

### Materials

[<sup>14</sup>C]glutamic acid and [<sup>3</sup>H]GABA were obtained from Amersham Pharmacia Biotech UK Ltd, Buckinghamshire, UK. D(-)-2-amino-5-phosphonopentanoic acid (AP-5), 6-cyano-7-nitroquinoxaline-2,3-dione-disodium (CNQX), 3,7-dimethyl-1-propargylxanthine (DMPX), dihydro-β-erythroidine hydrobromide (DHβE), and calmidazolium chloride were purchased from Research Biochemicals International (RBI), Natick, MA, USA. Adenosine 5'-triphosphate (ATP), adenosine 5'-diphosphate (ADP), pyridoxalphosphate-6-azophenyl-2',4'-disulfonic acid (PPADS), Brilliant blue G, adenosine 5'-triphosphate periodate oxidized (oxiATP), 2'- & 3'-O-(4-benzoyl-benzoyl)adenosine 5'-triphosphate (BzATP), ethylene-diamine tetraacetic acid (EDTA), gadolinium III (Gd<sup>3+</sup>), tetrodotoxin (TTX) (+/-)-nipecotic acid, and (aminoxy)acetic acid were obtained from Sigma Chemical Co., St Louis, MO, USA. 8,8'-(Carbonylbis(imino-4,1-phenylenecarbonylimino-4,1-phenylenecarbonylimino)) bis(1,3,5-naphthalenetrisulfonic acid) (NF279), Reactive Blue 2, and β-alanine were obtained from Tocris Cookson Ltd, Bristol, UK. Other compounds used: atropine sulfate (EGIS, Budapest, Hungary), 2'-(or-3')-O-(2,4,6-trinitrophenyl)adenosine 5'-triphosphate trisodium (TNP-ATP, Molecular Probes, Eugene, OR, USA), suramin (Bayer, Germany). Zinc as zinc sulfate salt (Reanal, Budapest, Hungary) was applied. GYKI 53655 was kindly provided by István Tarnawa (Richter Gedeon Pharmaceuticals, Budapest, Hungary). Calmidazolium chloride was dissolved in DMSO, the final concentration of DMSO was 0.018% v/v. DMPX was dissolved in 45% w/v solution of the inert compound 2-hydroxypropyl-β-cyclodextrin (RBI). Neither of the vehicles had significant effect on [<sup>3</sup>H]GABA release. The other compounds were dissolved in twice distilled water.

### *In situ* hybridization

Rats were anaesthetized with intraperitoneal sodium pentobarbitone (Sagatal 60 mg/mL, Rhone Merieux, Essex, UK) and perfused transcardially with sucrose containing artificial cerebrospinal fluid. Forebrain was removed and frozen on dry ice prior to storage at -80°C. Sections were cryostat cut at 10 μm, mounted on slides that had been pre-treated with 3-aminopropyltriethoxysilane (Sigma) and stored at -80°C until use. A 200 bp cDNA fragment of the P2X<sub>7</sub>R corresponding to bases from 127 to 328 (numbering according to accession no. X95882) was cloned into pGEM T-easy (Promega, Southampton, UK) and used to generate DIG-labelled sense and antisense RNA probes. *In situ* hybridization was carried out by a modified version of the manufacturer's protocol (<http://www.biochem.roche.com>). The sections were mounted in Aquamount and were viewed on a Nikon E600 microscope.

### Immunohistochemistry

Male rats (150–200 g, *n* = 5) were anaesthetized by intraperitoneal Sagatal (60 mg/kg) and transcardially perfused with fixative containing 4% paraformaldehyde and 0.1–0.5% glutaraldehyde in

0.1 M phosphate buffer (PB) pH 7.4. 50 µm coronal sections containing the hippocampus were cut at on a vibrating microtome (Leica, Milton Keynes, UK) and collected into phosphate-buffered saline (PBS) pH 7.2. The primary antibody used to detect the P2X<sub>7</sub>R was raised in rabbit against residues 576–595 of rat P2X<sub>7</sub>R with additional N-terminal cysteine (P2X<sub>7</sub>R Alomone Laboratories, Jerusalem, Israel) diluted 1 : 5000–1 : 15 000 in PBS, while that against parvalbumin was a mouse monoclonal antibody used at 1 : 1000 (Sigma). The procedures for light and electron microscopic immunohistochemistry have been described previously (Atkinson *et al.* 2000).

#### Specificity of the antibody

A BLAST search of the peptide sequence against which the primary antibody was raised resulted in hits only for the P2X<sub>7</sub> receptor. In addition this sequence lies in the C-terminal portion of the P2X<sub>7</sub> receptor which is longer than that of other P2X receptors and is therefore not present in other P2X receptors (Surprenant *et al.* 1996). Western blotting of rat brain tissue revealed that the antibody recognizes a protein of molecular weight appropriate for the P2X<sub>7</sub> receptor (Deuchars *et al.* 2001; Kim *et al.* 2001). As further controls, sections were incubated in PBS in place of primary antiserum for 12–24 h at 4°C, or in primary antiserum which had been pre-absorbed with peptide antigen for 1 h before use (1 µg of peptide for 1 µg of antibody) immunoreactivity was then visualised with peroxidase or fluorescent procedures. There was no staining with either control procedures. Taken together, these data indicate that the antibody specifically recognises the P2X<sub>7</sub> receptor.

#### Double-labelling studies

P2X<sub>7</sub> immunoreactivity was detected with peroxidase-based methods and sections were then incubated in anti-parvalbumin antibody for 12–24 h at 4°C. Sections were then washed 3 × 10 min in PBS, and then incubated in secondary antibody to mouse IgG conjugated to 1 nm gold particles (Amersham Life Sciences, Buckinghamshire, UK) diluted 1 : 200 in PBS pH 7.4 containing 0.8% fish gelatine and 1% bovine serum albumin for 18–24 h at 4°C. Sections were rinsed in PBS (3 × 10 min) followed by a 10 min wash in PBS containing 2% glutaraldehyde, the sections were then thoroughly rinsed (4 × 10 min) in distilled deionized water (DDW) and the gold particles were silver enhanced for 5–10 min using an Intense silver enhancement kit (Amersham Life Sciences). Sections were then prepared for light and electron microscopy (EM) as described previously (Atkinson *et al.* 2000). For presentation, EM negatives were digitised using an Agfa Duoscan Scanner and manipulated in Corel Draw 9 to adjust gamma, brightness and contrast levels.

#### Fluorescence light microscopy

Tissue sections were obtained as above and incubated in rabbit anti P2X<sub>7</sub>R as above at a concentration of 1 : 3000–1 : 5000 in PBS with 0.1% Triton. Following 3 × 10-min washes in PBS, sections were transferred to PBS containing Cy3 conjugated anti-rabbit (Jackson ImmunoResearch, Stratech, Luton, UK) at 1 : 1000 for 4–12 h. Sections were then washed three times in PBS, dried onto gelatin-coated slides at 4°C and mounted in Vectamount. For double-labelling with parvalbumin, P2X<sub>7</sub>R immunoreactivity was detected with Cy3 as described above. Sections were then incubated in anti-parvalbumin primary antibody for 18–24 h at 4°C. After washing in

PBS for 3 × 10 min, the sections were then incubated in a mouse biotinylated secondary antibody (1 : 200 in PBS, Vector Laboratories, Burlingame, CA, USA) for 4 h at room temperature. The sections were then washed for 3 × 10 min in PBS before incubation in streptavidin ALEXA (1 : 1000 in PBS, Molecular Probes, Eugene, OR, USA) for 2 h at room temperature. Sections were then washed three times in PBS, dried onto slides and mounted in Vectamount. Images were captured directly from the slide using an Aquis Image Capture system, and contrast, brightness and gamma were adjusted in Corel Draw 9.

#### Statistics

All data represent mean ± SEM of *n* observations. EC<sub>50</sub> and IC<sub>50</sub> values were calculated by fitting the data to sigmoidal logistic equations using the program Prism (Graph Pad, San Diego, CA, USA). Statistical significance was calculated by Student's *t*-test, Welch's test, one or two-way ANOVA followed by Dunnett's test, as appropriate, and *p* < 0.05 was accepted as significant change.

## Results

### P2X<sub>7</sub> receptor activation evoked [<sup>3</sup>H]GABA release from rat hippocampal slices

After 60 min preperfusion, the spontaneous tritium efflux in the first 3-min sample was 0.193 ± 0.021% (*n* = 6) of the total actual tissue tritium content, and remained fairly constant until the end of the experiment. When the slices were challenged to 1 min perfusions of ATP of increasing concentrations, a dose-dependent elevation in the basal tritium outflow was observed in the 1–30 mM concentration range, which was reversible upon washout (Fig. 1a,b). Although maximal effect was not obtained in this concentration range, because of potential non-specific effects, higher concentrations were not evaluated, and therefore EC<sub>50</sub> values could not be calculated. This unsaturable feature is characteristic to a number of P2X receptor-mediated responses (see e.g. Kennedy and Leff 1995; Visentin *et al.* 1999; Hibell *et al.* 2001). The net tritium release evoked by 10 mM ATP (*S*<sub>ATP1</sub> = 0.181 ± 0.037%; *n* = 12) was comparable to that obtained by electrical field stimulation and was reproducible upon a subsequent identical stimulus resulting in an *S*<sub>ATP2</sub>/*S*<sub>ATP1</sub> ratio of 1.03 ± 0.12% (*n* = 12, see also Fig. 3a). Although this concentration of ATP changed the Ca<sup>2+</sup> concentration of the solution from 2.5 mM to 0.62 mM, and altered Ca<sup>2+</sup>/Mg<sup>2+</sup> ratio in the Krebs' solution may change neuronal excitability, if we restored the Ca<sup>2+</sup> concentration of the solution no change in ATP-evoked [<sup>3</sup>H]GABA efflux was observed (*S*<sub>ATP2</sub>/*S*<sub>ATP1</sub> = 0.82 ± 0.051 at 2.5 mM [Ca<sup>2+</sup>]). When the Ca<sup>2+</sup> concentration of the solution was decreased to 0.62 mM by the calcium chelator EDTA, an increase was detected in [<sup>3</sup>H]GABA outflow (0.020 ± 0.004%), but its amount could be accounted for not more than 16.7 ± 0.3% of the effect of ATP. As relatively high concentrations of ATP

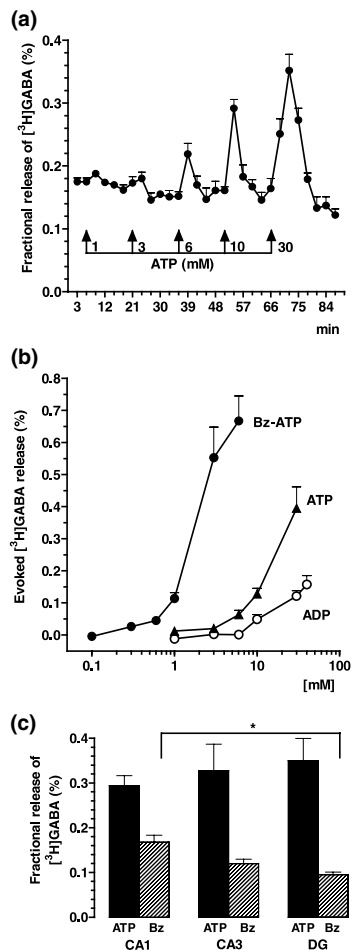


**Fig. 1** Effect of P2 agonists on the release of  $[^3\text{H}]\text{GABA}$  from hippocampal slices. (a) Concentration-dependent effect of ATP (1–30 mM). The release of  $[^3\text{H}]\text{GABA}$  was expressed as a fractional release (%), for calculation see Materials and methods) and is shown as a function of time. Arrows show 1 min long ATP perfusions at the concentrations (in mM) indicated. The perfusion solution contained CNQX (10  $\mu\text{M}$ ) and AP-5 (10  $\mu\text{M}$ ). (b) Concentration–response curves of three P2 agonists. Following the protocol showed in Fig. 1, slices were perfused for 1 min with agonists at increasing concentrations: ATP (1–30 mM,  $\blacktriangle$ ), BzATP (0.1–6 mM,  $\bullet$ ), and ADP (1–40 mM,  $\circ$ ). The release of  $[^3\text{H}]\text{GABA}$  is expressed as fractional release (%) and the agonist-evoked release of  $[^3\text{H}]\text{GABA}$  was calculated by the AUC method (for details see Materials and methods). The values show mean  $\pm$  SEM of four identical experiments. (c) Subregional distribution of the effect of ATP and BzATP in the hippocampus. The three major subregions, i.e. CA1 region (CA1), CA3 region (CA3), and dentate gyrus (DG) were individually isolated and used in  $[^3\text{H}]\text{GABA}$  release experiments, as described above. ATP (ATP, 10 mM)- and BzATP (Bz, 1 mM)-evoked release was calculated by the AUC method ( $n = 3$ ); \* $p < 0.05$  vs. CA1.

were required to release  $[^3\text{H}]\text{GABA}$ , indicative for the involvement of P2X<sub>7</sub>-like purinoceptors, the effect of other agonists acting at this particular subtype, i.e. BzATP (0.1–6 mM), and ADP (1–40 mM) were also assessed (Fig. 1b).

BzATP was active in a concentration range almost one order of magnitude lower than ATP, whereas ADP was found to be a weak agonist. Thus the rank order of agonist potency to evoke tritium outflow was BzATP  $\gg$  ATP  $>$  ADP. To explore regional differences in the effect of P2X agonists to release  $[^3\text{H}]\text{GABA}$ , CA1, CA3 and DG subregions of the hippocampus were separated and were exposed to 10 mM ATP and 1 mM BzATP for 1 min. The resting  $[^3\text{H}]\text{GABA}$  outflow was similar, and both ATP (10 mM) and BzATP (1 mM) were active to release  $[^3\text{H}]\text{GABA}$  in all three subregions (Fig. 1c). Although BzATP released significantly higher amount of  $[^3\text{H}]\text{GABA}$  from CA1 than from DG (Fig. 1c,  $p < 0.05$ ), the difference between the two regions was not marked.

In subsequent experiments, the effect of different P2 receptor antagonists and divalent cations were evaluated on the action of ATP (1–30 mM), using the protocol described above. As illustrated in Fig. 2, Brilliant blue G (100 nM; Fig. 2a), an antagonist, reported to be selective for P2X<sub>7</sub>Rs with nanomolar affinity (Jiang *et al.* 2000), the relatively P2X<sub>7</sub>-selective oxidized ATP (oxiATP; 300  $\mu\text{M}$ ; Fig. 2c), and the non-selective P2 antagonist PPADS (30  $\mu\text{M}$ ; Fig. 2c) all depressed the effect of ATP at several ATP concentrations tested, whereas suramin (300  $\mu\text{M}$ ) facilitated rather than inhibited the action of 30 mM ATP (Fig. 2c). The inhibitory action of Brilliant blue G and PPADS was also tested on 10 mM ATP-evoked release of  $[^3\text{H}]\text{GABA}$ , according to the protocol shown in Fig. 3(a). The inhibitory effect of Brilliant blue G was concentration-dependent between 1 and 100 nM, with an IC<sub>50</sub> value of  $1.6 \pm 1.0$  nM (Fig. 3b) and the maximal inhibitory effect of Brilliant blue G was observed at 100 nM ( $44 \pm 6\%$ ;  $n = 4$ ). PPADS also reduced 10 mM ATP-evoked release of  $[^3\text{H}]\text{GABA}$  in a concentration-dependent manner within the concentration range of 3 and 30  $\mu\text{M}$ , with an IC<sub>50</sub> value of  $6.8 \pm 2.2$   $\mu\text{M}$ , and the maximal inhibitory effect of PPADS was observed at 30  $\mu\text{M}$  ( $52 \pm 3\%$ ,  $n = 8$ ). Hence, Brilliant blue G was more than 1000-fold more potent than PPADS in antagonising the effect of ATP. Other P2-antagonists, i.e. TNP-ATP (30  $\mu\text{M}$ ), NF279 (2  $\mu\text{M}$ ), and Reactive Blue 2 (20  $\mu\text{M}$ ) did not significantly shift the dose–response curve of ATP (Fig. 2b). Because divalent cations (e.g. Zn<sup>2+</sup>, Mg<sup>2+</sup>) have a differential action on the agonist activity at different P2X receptor subtypes, the effect of ATP was also examined in the absence of external Mg<sup>2+</sup> (Fig. 2a) and in the presence of Zn<sup>2+</sup> (0.1–30  $\mu\text{M}$ , Fig. 3b). Lack of Mg<sup>2+</sup> in the Krebs' solution potentiated the 6 and 10 mM ATP-evoked  $[^3\text{H}]\text{GABA}$  release by  $88 \pm 20\%$  and by  $80 \pm 18\%$ , respectively ( $n = 4$ ,  $p < 0.05$ ; Fig. 2a). In contrast, Zn<sup>2+</sup> (0.1–30  $\mu\text{M}$ ), which has a potentiating action on several P2X subtypes but is an inhibitor of P2X<sub>7</sub>R (Virginio *et al.* 1997), concentration-dependently inhibited the action of ATP (10 mM; Fig. 3b), with the IC<sub>50</sub> of  $0.29 \pm 0.18$   $\mu\text{M}$ , and with the maximal inhibition of  $55.4 \pm 8.2\%$  at 30  $\mu\text{M}$  ( $p < 0.05$ ).

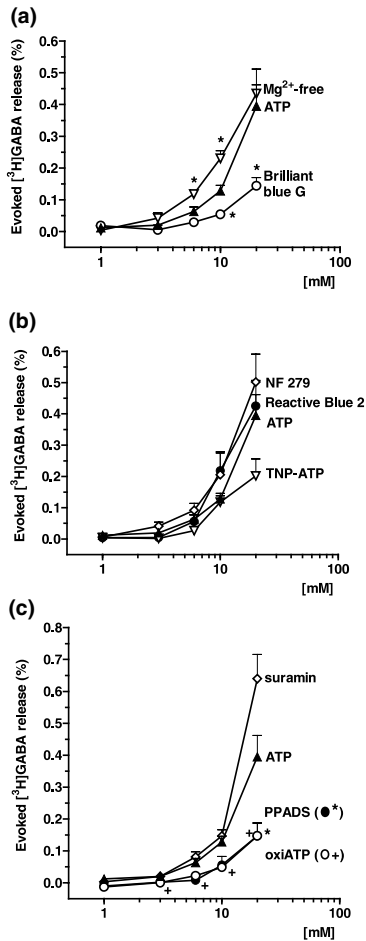


**Fig. 2** Concentration–response curve of ATP in the presence of some P2 antagonists, and in lack of Mg<sup>2+</sup>. Following the protocol showed in Fig. 1, ATP (1–30 mM, ▲) was perfused for 1 min in the presence of (a), Brilliant blue G (100 nM, ○) and Mg<sup>2+</sup>-free conditions (△); (b), NF 279 (2 μM, ◇), Reactive Blue 2 (20 μM, ●), and TNP-ATP (30 μM, △); (c) suramin (300 μM, ◇), PPADS (30 μM, ●, \* indicates the significant difference from control,  $p < 0.05$ ) and oxidized ATP (300 μM, ○, \* indicates the significant difference from control,  $p < 0.05$ ). All antagonists, and Mg<sup>2+</sup>-free Krebs' solution were introduced 10 min prior to the sample collection period. Perfusion of oxATP started 2 h prior to the collection of samples. ▲, control. All data represent mean ± SEM of four identical experiments except the experiment with suramin ( $n = 8$ ).

The possible participation of other facilitatory receptors expressed on GABAergic neurones mediating the effect of ATP was tested using the muscarinic acetylcholine receptor blocker atropine (1 μM), the nicotinic receptor antagonist dihydro-β-erythroidine (DHβE, 10 μM) and the adenosine receptor antagonist DMPX (250 nM), which were perfused 15 min before S<sub>ATP2</sub>. None of these drugs affected the action of ATP (10 mM) to release [<sup>3</sup>H]GABA (S<sub>ATP2</sub>/S<sub>ATP1</sub> = 0.96 ± 0.12 for atropine, 1.09 ± 0.23 for DHβE and 1.24 ± 0.26 for DMPX;  $n = 4$ ,  $p > 0.05$  vs. control).

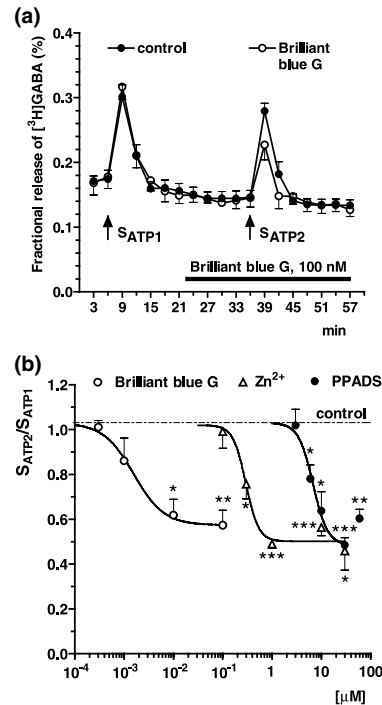


**Fig. 3** Concentration-dependent effect of PPADS, Zn<sup>2+</sup> and Brilliant Blue G on ATP-evoked release of [<sup>3</sup>H]GABA. A, ATP (10 mM) was perfused twice for 1 min (as indicated by arrows), 6 (S<sub>ATP1</sub>) and 36 (S<sub>ATP2</sub>) min after the beginning of the sample collection period. ○, Data from experiments when Brilliant blue G (100 nM) was applied 15 min before S<sub>ATP2</sub>. ●, Identical experiments without Brilliant blue G perfusion (control). (b) S<sub>ATP2</sub>/S<sub>ATP1</sub> values for PPADS (1–60 μM, ●), Zn<sup>2+</sup> (0.1–30 μM, △) and Brilliant blue G (0.3–100 nM, ○) yielded inhibitory dose–response curves (for PPADS the curve was calculated in the concentration range from 1 to 30 μM). Every point represents mean ± SEM of 4–12 identical experiments. Asterisks indicate significant differences from control: \* $p < 0.05$ ; \*\* $p < 0.01$ ; \*\*\* $p < 0.001$ .

Although P2X<sub>7</sub>R has previously been suggested to be expressed in activated microglia and ependymal cells in the adult rat brain (Collo *et al.* 1997), the release studies indicated that activation of the P2X<sub>7</sub>R could result in the release of GABA and we therefore sought to determine the structures that could be involved in the hippocampus.

### Neuronal expression of the P2X<sub>7</sub>R in the hippocampal formation

P2X<sub>7</sub>R messenger RNA (mRNA) was present in the cytoplasm of neurones in the granule cell layer as well as the stratum pyramidale of the CA1 and CA3 regions (Fig. 4a). A positive reaction was observed only in sections hybridized with antisense and not in sections incubated with a sense probe or without a probe (Fig. 4b). Because *in situ* hybridization revealed neuronal expression, we tested for the presence of the P2X<sub>7</sub>R protein using immunohistochemistry.

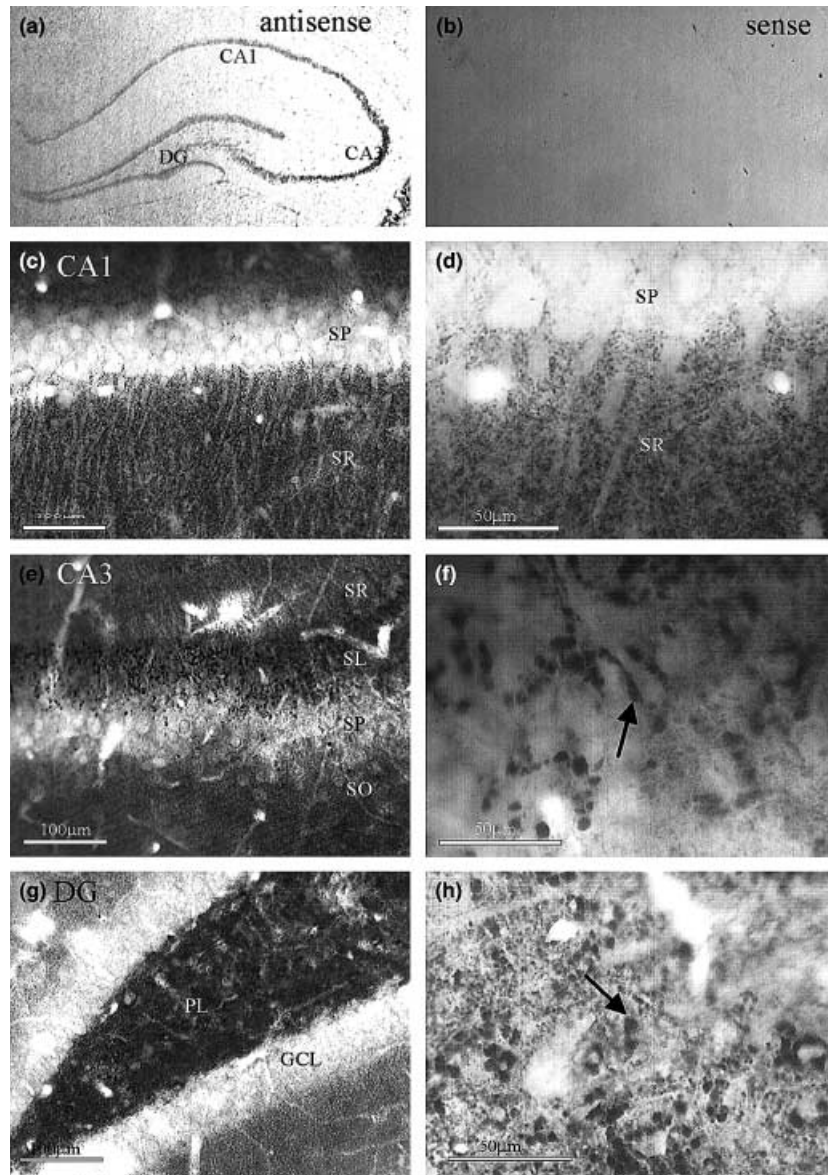


**Fig. 4** P2X<sub>7</sub>R mRNA expression and P2X<sub>7</sub>R immunoreactivity (P2X<sub>7</sub>-IR) in the hippocampus. (a) *In situ* hybridization reveals that messenger RNA coding for the P2X<sub>7</sub>R is present throughout the cell body layers of the hippocampus, including stratum pyramidale in the CA1 and CA3 regions as well as the granule cell layer in the dentate gyrus (DG). Section from the hippocampus indicating positive signal following hybridization with a DIG-labelled antisense probe specific to the P2X<sub>7</sub>R, visualised with alkaline phosphatase. (b) Section of the hippocampus indicating lack of signal when tissue was incubated with a sense probe to the P2X<sub>7</sub>R. All incubations and reactions were carried out alongside those with the antisense probe. (c) P2X<sub>7</sub>R immunoreactivity is located in terminal fields in the hippocampus. Low power magnification of the CA1 region. P2X<sub>7</sub>R immunoreactivity is localised to numerous punctate structures in the stratum radiatum (SR). In contrast, the stratum pyramidale (SP) is almost devoid of labelling. (d)

Higher magnification of an area of the CA1 region. The P2X<sub>7</sub>-R immunoreactive punctate structures appear to outline dendrites in the stratum radiatum, but the dendrites themselves are immunonegative. (e) In the CA3 region the stratum lucidum (SL) contained dense punctate immunoreactivity, but labelling in the stratum pyramidale was sparse. SO: stratum oriens. (f) At higher magnification the labelling in stratum lucidum can be observed in punctate structures of approximately 5 µm diameter. The arrow indicates one such example. (g) In the dentate gyrus the granule cell body layer (GCL) is devoid of labelling. In contrast heavy labelling is observed in the polymorphic layer (PL). (h) Higher magnification of the polymorphic layer of the dentate gyrus illustrating that the dense immunoreactivity is the result of numerous labelled punctate structures, an example of which is indicated by the arrow.

### P2X<sub>7</sub>R immunoreactivity in excitatory terminal fields of the hippocampal formation

Immunoprodukt for the P2X<sub>7</sub>R was found in terminal fields that were characteristic of the major excitatory pathways in the hippocampus (Fig. 4c–h). These labelled terminal fields were particularly obvious with respect to the giant mossy fibre terminals in stratum lucidum of the CA3 region (Fig. 4e,f) and the dentate gyrus (Fig. 4g,h). Labelling was also observed in the stratum radiatum and stratum oriens of the CA1 region (Fig. 4c,d). The cell body layers in the hippocampus generally did not contain any somatic labelling (Fig. 4c,e,g) and very few punctate structures (Fig. 4d).

In tissue sections double-labelled for parvalbumin, P2X<sub>7</sub>R immunoreactivity was not co-localized with parvalbumin (Fig. 5). This was most obvious in the dentate gyrus (Fig. 5b) and stratum lucidum of the CA3 region (Fig. 5a,c,d).

Electron microscopic examination revealed that P2X<sub>7</sub>R immunoreactivity was predominantly present in presynaptic terminals that formed asymmetric-type synaptic contacts consistent with excitatory synapses (Fig. 6). Within each labelled terminal, the diaminobenzidine (DAB) reaction product was most often highly localized to one region of the terminal (Fig. 6). In some cases the labelling was present at the face of the presynaptic membrane (Fig. 6f), but also appeared distant from the active zone (Fig. 6a,c). Labelling

was present in large terminals that were probably mossy fibre terminals in stratum lucidum of the CA3 region (Fig. 6c,d) and the DG (Fig. 6e,f). In the CA1 region, immunoreactivity was observed in smaller terminals in the stratum oriens and stratum radiatum (Fig. 6a,b). These terminals most often made synaptic contacts with dendritic spines (Fig. 6a,b), but also dendritic shafts.

Although activation of the P2X<sub>7</sub>R induced release of GABA, our anatomical studies suggested that the P2X<sub>7</sub>R was localised to excitatory terminals. We therefore addressed the question if the GABA release could be due to P2X<sub>7</sub>R containing terminals impinging onto inhibitory interneurons. In sections that had been double-labelled to reveal immunoreactivity for parvalbumin (a calcium-binding protein found in a subset of hippocampal interneurons) and the P2X<sub>7</sub>R, P2X<sub>7</sub>R immunoreactive terminals did indeed innervate parvalbumin immunoreactive dendrites in the areas examined (CA3 and CA1, Fig. 6a,c).

### The role of excitatory amino acid-mediated transmission in the effect of ATP

Because P2X<sub>7</sub>R immunoreactivity was localized to excitatory terminals in the hippocampus we examined the possibility that excitatory amino acid (EAA)-mediated transmission is involved in [<sup>3</sup>H]GABA release evoked by ATP. The voltage-dependent Na<sup>+</sup> channel blocker TTX

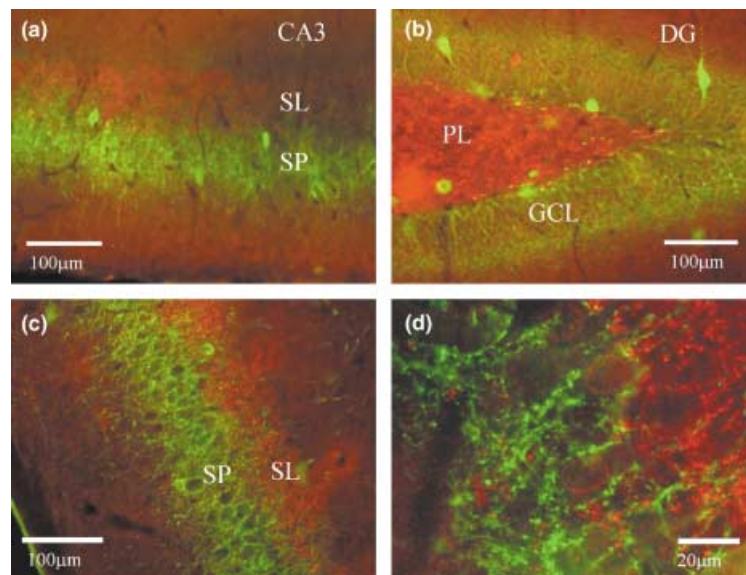


**Fig. 5** P2X<sub>7</sub>R immunoreactivity is not colocalised with parvalbumin immunoreactivity. (a) Fluorescence image indicating that parvalbumin immunoreactivity is dense in the stratum pyramidale (SP) in CA3 where it labels fibres and occasional somata (green) while P2X<sub>7</sub>R immunoreactivity (red) is dense in stratum lucidum (SL). (b) Parvalbumin immunoreactivity in the dentate gyrus is dense in the granule cell layer (GCL), where numerous labelled cell fibres and occasional cell body can be observed (green). The distribution of P2X<sub>7</sub>R immuno-

reactivity contrasts with that of the parvalbumin-IR since staining (in red) is dense in the polymorphic cell layer (PL) but absent from the granule cell layer (GCL). There are no examples of colocalisation. (c) Another example of the contrasting patterns of parvalbumin staining (green) in the CA3 region with that of P2X<sub>7</sub>R labelling (red) in the stratum lucidum (SL). (d) Higher magnification of a portion of the CA3 region revealing that parvalbumin (green) and P2X<sub>7</sub>R (red) immunoreactivity are not co-localized.

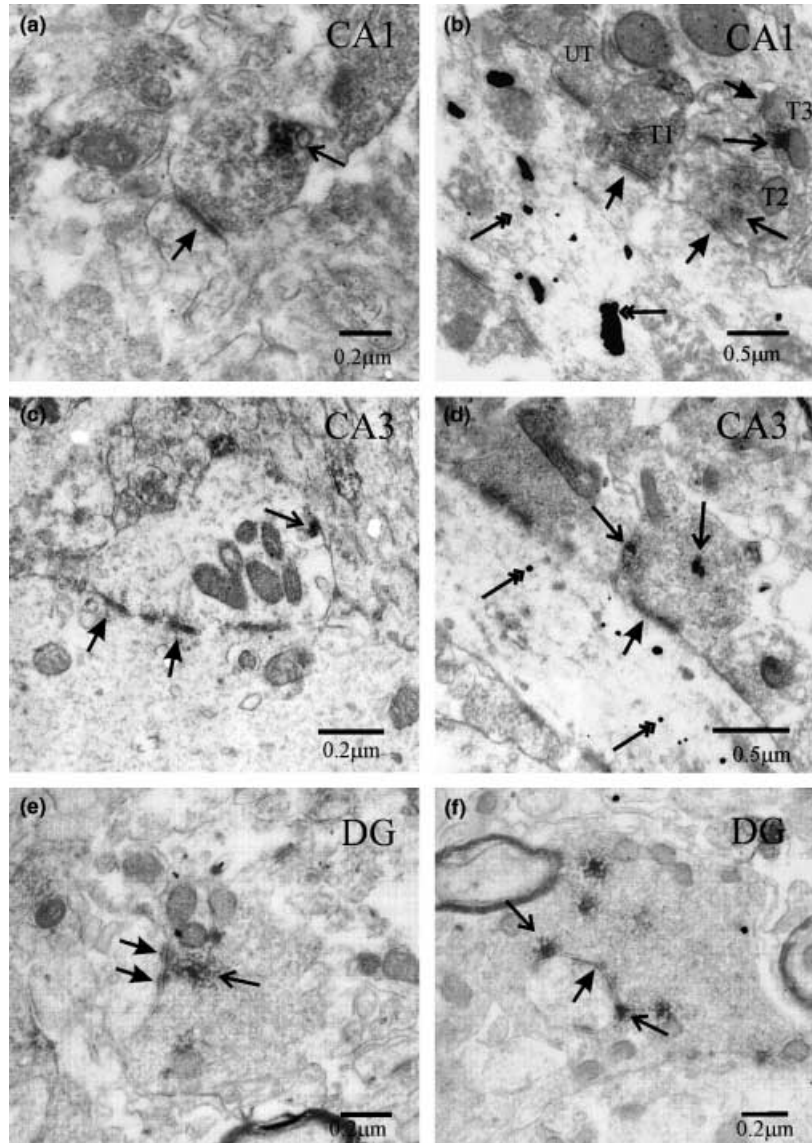


**Fig. 6** Electron microscopy reveals that P2X<sub>7</sub>R immunoreactivity is present in synaptic terminals including those that innervate parvalbumin containing structures. In all micrographs P2X<sub>7</sub>R immunoreactivity is identified by DAB reaction product (open ended arrows) is present in presynaptic terminals which form synaptic specializations (indicated by closed-head arrows) with dendritic shafts (a,c,d,e,f) or dendritic spines (a,b) while parvalbumin containing structures are identified by gold particles (double-headed open arrows). In CA3 (c,d) and dentate gyrus (DG; e,f) immunoreactivity is present in large terminals resembling those of mossy fibres. In CA1 (a,b) P2X<sub>7</sub>R-IR

terminals are smaller and display morphology associated with asymmetric type of synapse. (b) Two P2X<sub>7</sub>R-IR terminals in CA1 region (T1 and T2; identified by DAB, open-head arrows) form synaptic contacts (arrows) with a parvalbumin containing dendrite (gold particles, double open-headed arrows). Another terminal (T3) is in synaptic contact with an unlabelled dendritic spine (d). A terminal in CA3 region containing immunoreactivity for the P2X<sub>7</sub>R (open-head arrow) forms a synaptic contact (arrow) with the dendritic shaft of a parvalbumin containing dendrite (identified by gold particles, double open-headed arrows).

(1 μM) strongly decreased [<sup>3</sup>H]GABA efflux evoked by 10 mM ATP (Fig. 7a), indicating that the effect of ATP is sodium-dependent and its initiation site is located upstream from action potential generation. Although AP-5 (10 μM), an NMDA receptor antagonist, and CNQX (10 μM), the AMPA receptor antagonist, were routinely included into the perfu-

sion solution, recent observations suggest that kainate receptors are also involved in excitatory transmission in the hippocampus and they are inhibited only by higher concentrations of CNQX than 10 μM (Castillo *et al.* 1997). Indeed, when the concentration of CNQX was elevated, a dose-dependent (10–100 μM) and significant reduction in the

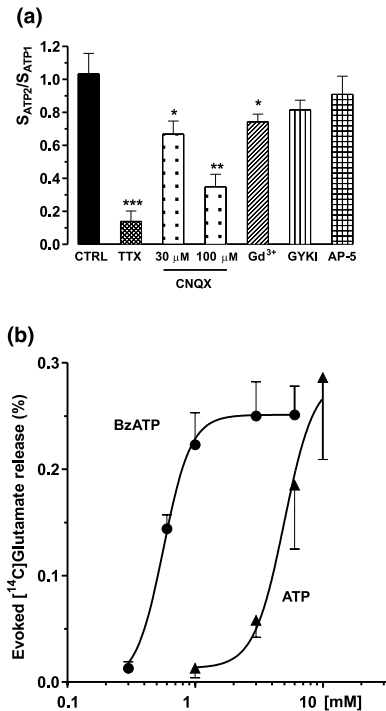


**Fig. 7** (a) Tetrodotoxin (TTX, 1  $\mu$ M,  $n = 4$ ), increasing the concentration of CNQX (30 and 100  $\mu$ M,  $n = 4$ –4), and the selective kainate antagonist gadolinium ion (Gd<sup>3+</sup>, 100  $\mu$ M,  $n = 4$ ) reduced the effect of ATP to release [<sup>3</sup>H]GABA, whereas the highly selective AMPA antagonist GYKI 53655 (GYKI, 20  $\mu$ M,  $n = 4$ ) and the NMDA type glutamate receptor blocker AP-5 (50  $\mu$ M,  $n = 7$ ) did not significantly affect the action of ATP (black bar, CTRL). The effect of drugs is expressed as  $S_{ATP_2}/S_{ATP_1}$  values, in experiments performed according to the protocol shown in Fig. 3(a). Asterisks indicate significant differences from control: \* $p < 0.05$ ; \*\* $p < 0.01$ ; \*\*\* $p < 0.001$ . (b) Concentration-dependent effect of ATP (1–10 mM,  $n = 9$ ,  $\blacktriangle$ ) and BzATP (0.6–6 mM,  $n = 5$ ,  $\bullet$ ) on the release of [<sup>14</sup>C]glutamate. Experiments were performed according to the protocol shown in Fig. 1(a).

effect of ATP to release GABA was observed (Fig. 7a), indicating that kainate receptor-mediated transmission might be partly involved in this action. The maximal inhibition obtained by 100  $\mu$ M CNQX was  $66 \pm 7\%$ . To confirm this assumption the effect of selective AMPA receptor antagonist GYKI 53655 (20  $\mu$ M) and the selective kainate receptor antagonist Gd<sup>3+</sup> (100  $\mu$ M) were also examined. Whereas GYKI 53655 did not affect significantly [<sup>3</sup>H]GABA efflux, Gd<sup>3+</sup>, at a concentration selective for kainate receptor (100  $\mu$ M) decreased the response (Fig. 7a). In contrast, no change in the effect of ATP was detected when the concentration of the effect of the NMDA receptor-blocker AP-5 was elevated to 50  $\mu$ M (Fig. 7a).

In order to obtain further proof of the involvement of EAA transmission in the effect of ATP, it was also examined whether activation of P2X<sub>7</sub> receptors could indeed promote glutamate release. Hippocampal slices were pre-loaded with

[<sup>14</sup>C]glutamic acid and then [<sup>14</sup>C]efflux was measured as an indicator of glutamate release. The basal efflux of [<sup>14</sup>C]glutamate was  $0.16 \pm 0.02\%$  ( $n = 14$ ). ATP (1–10 mM), and BzATP (0.3–6 mM), administered according to an identical protocol to that used in case of [<sup>3</sup>H]GABA release experiments (Fig. 1a), elicited a concentration-dependent increase in [<sup>14</sup>C]glutamate level in the effluent (Fig. 7b). The concentration range in which the two ATP analogues promoted [<sup>14</sup>C]glutamate efflux was somewhat lower than that observed in case of [<sup>3</sup>H]GABA efflux, and among them BzATP was clearly more potent ( $EC_{50}$  values for BzATP and ATP were  $564 \pm 32 \mu$ M and  $5.0 \pm 0.9$  mM, respectively). The maximal effect obtained by ATP was  $0.286 \pm 0.077\%$ , similar to that obtained by BzATP ( $0.251 \pm 0.027\%$ ,  $n = 9$  and 5).

### Subcellular mechanism underlying the effect of ATP

In the following set of experiments we addressed the question whether extracellular GABA accumulation in response to ATP is an exocytotic process or due to the reversal of the GABA transporter present on the nerve terminal membrane. To distinguish between carrier-mediated and exocytotic release of GABA, the bath temperature was fast cooled to 12°C, 15 min before the second ATP perfusion, as at low temperature (< 17°C) the integral transporter proteins of cell membrane are inactivated, and only the Ca<sup>2+</sup>-dependent exocytotic release process remains functional (Vizi 1998). This was also shown for [<sup>3</sup>H]GABA release in our previous study using identical experimental conditions (Vizi and Sperlagh 1999). The resting outflow of tritium was  $0.167 \pm 0.008\%$  at 12°C ( $n = 4$ ,  $p > 0.05$ ). In contrast, this procedure almost completely abolished the [<sup>3</sup>H]GABA release evoked by 10 mM ATP (Fig. 8a). In addition, the effect of the selective GABA uptake inhibitor nipecotic acid (1 mM) was also examined, which is taken up preferentially by all GABA transporter types instead of GABA and inhibits GABA uptake into brain slices by 99% at this concentration (Krogsgaard-Larsen and Johnston 1975; Bahena-Trujillo and Arias-Montano 1999). When 1 mM nipecotic acid was perfused during the pre-perfusion period, the resting and electrical stimulation-evoked release of tritium was higher than in control experiments ( $5.09 \pm 0.41\%$ ,  $n = 4$ ,  $p < 0.001$ , and  $0.511 \pm 0.069\%$ ,  $n = 4$ ,  $p < 0.05$ , Fig. 8b) indicating an effective blockade of the uptake process. Under this condition 10 mM ATP did not evoke a detectable release of [<sup>3</sup>H]GABA (Fig. 8b). Calmidazolium (100 nM), which inhibits selectively P2X<sub>7</sub>R-mediated inward currents but not pore formation at recombinant P2X<sub>7</sub>Rs (Virginio *et al.* 1997), attenuated the effect of 10 mM ATP by  $43 \pm 5\%$  ( $n = 4$ ,  $p < 0.01$ ; Fig. 8a).

### The role of P2X<sub>7</sub>R activation by endogenous ATP

To study the role of P2X<sub>7</sub>R activation by endogenous ATP in excitatory synaptic transmission and subsequent GABA

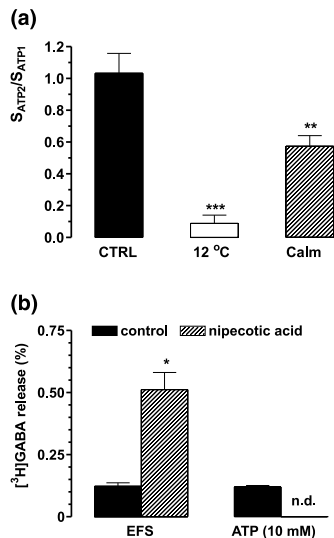


**Fig. 8** Mechanisms underlying the effect of ATP on  $[^3H]GABA$  release from hippocampal slices. (a) Effect of low bath temperature ( $12^{\circ}C$ , open bar,  $n = 4$ ), and Calmidazolium (Calm,  $100\text{ nM}$ ,  $n = 4$ , diagonally striped bar) on the ATP-evoked  $[^3H]GABA$  release. All treatments were applied 15 min before  $S_{ATP2}$ , and their effect was expressed as  $S_{ATP2}/S_{ATP1}$  ratios. Black bar (CTRL, black bar,  $n = 12$ ) represents control  $S_{ATP2}/S_{ATP1}$  value according to the protocol shown in Fig. 3(a). (b) Effect of the GABA uptake inhibitor nipecotic acid ( $1\text{ mM}$ ). After 60 min long perfusion of the slices with nipecotic acid electrical field stimulation (EFS,  $35\text{ V}$ ,  $10\text{ Hz}$ ,  $1\text{ ms}$ ) or 1 min long ATP ( $10\text{ mM}$ ) perfusion were applied. Black bars: evoked release by EFS and ATP in the absence of nipecotic acid, diagonally striped bars: EFS- and ATP-evoked release in the presence of nipecotic acid ( $n = 4\text{--}4$ , \* $p < 0.05$ ; \*\* $p < 0.01$ ; \*\*\* $p < 0.001$ , n.d. not detectable).

release from GABAergic target neurones, the effect of P2 receptor antagonists was examined on the release of  $[^3H]GABA$  evoked by neuronal activity mimicked by high-frequency electrical field stimulation (EFS;  $35\text{ V}$ ,  $10\text{ Hz}$ ,  $1\text{ ms}$ ,  $360$  pulses). Two identical periods of EFS, applied 6 and 36 min after the beginning of the collection period (EFS<sub>1</sub> and EFS<sub>2</sub>), resulted in a rapid and reproducible increase of the basal tritium efflux; the evoked-release elicited by EFS<sub>1</sub> and EFS<sub>2</sub> was  $0.198 \pm 0.018\%$  and  $0.182 \pm 0.02\%$ , respectively, giving an EFS<sub>2</sub>/EFS<sub>1</sub> ratio of  $0.92 \pm 0.04$  ( $n = 6$ ) under control conditions (Fig. 9a). Inhibition of axonal action potential propagation by tetrodotoxin (TTX,  $1\text{ }\mu\text{M}$ ) 15 min prior to EFS<sub>2</sub> almost completely abolished EFS-evoked tritium release (EFS<sub>2</sub>/EFS<sub>1</sub> =  $0.12 \pm 0.07\%$ ,  $n = 6$ ;  $p < 0.001$ ) indicating that it is the result of the axonal activity. Brilliant blue G ( $100\text{ nM}$ ), the P2X<sub>7</sub>R-selective antagonist, decreased the EFS<sub>2</sub>/EFS<sub>1</sub> ratio by  $32 \pm 5\%$  ( $n = 8$ ,  $p < 0.01$ ). Similarly to Brilliant blue G, PPADS ( $30\text{ }\mu\text{M}$ ) also reduced significantly the EFS-evoked release of  $[^3H]GABA$  by  $39 \pm 8\%$  ( $n = 6$ ,  $p < 0.01$ ; Fig. 9b). When the bath temperature was lowered to  $12^{\circ}C$ , the EFS-evoked release was decreased by  $57 \pm 6\%$  ( $n = 4$ ,  $p < 0.01$  vs.  $37^{\circ}C$ ). Under

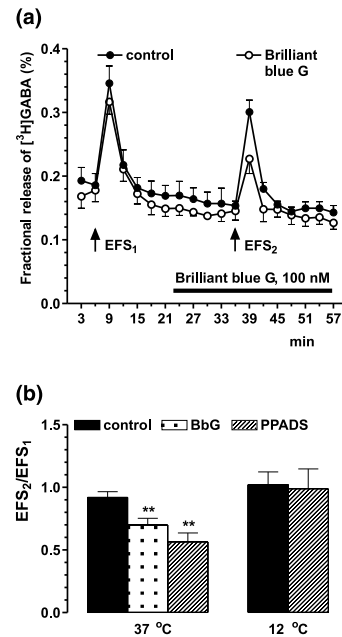


**Fig. 9** (a) Brilliant Blue G ( $100\text{ nM}$ ) attenuates electrically evoked release of  $[^3H]GABA$ . Electrical field stimulation ( $35\text{ V}$ ,  $10\text{ Hz}$ ,  $1\text{ ms}$ ,  $360$  shocks) were applied 6 (EFS<sub>1</sub>) and 36 (EFS<sub>2</sub>) min after the beginning of the sample collection period as indicated by arrows. ●, Data from control experiments ( $n = 6$ ); ○, data from experiments when Brilliant Blue G ( $100\text{ nM}$ ) was applied 15 min before EFS<sub>2</sub> ( $n = 6$ ). (b) The effect of Brilliant Blue G (BbG,  $100\text{ nM}$ ) and PPADS ( $30\text{ }\mu\text{M}$ ) on evoked release of  $[^3H]GABA$ . Low bath temperature ( $12^{\circ}C$ , the bath temperature was decreased to  $12^{\circ}C$  15 min before EFS<sub>1</sub>) prevent the effect of PPADS to attenuate electrically evoked release of  $[^3H]GABA$ . The results are expressed as EFS<sub>2</sub>/EFS<sub>1</sub> values obtained from the experiments illustrated in Fig. 9(a). All bars represent mean  $\pm$  SEM from six experiments. Asterisks indicate significant differences from respective control: \* $p < 0.05$ , \*\* $p < 0.01$ .

these conditions the effect of PPADS on EFS-evoked release of  $[^3H]GABA$  was no longer detected (Fig. 9b).

## Discussion

Our findings demonstrate that P2X<sub>7</sub>Rs: (i) are located on excitatory nerve terminals of CA1, CA3 and dentate gyrus region of hippocampus innervating both excitatory and inhibitory cells and (ii) their activation regulate the efflux of glutamate and GABA, released from excitatory nerve terminals as well as from their inhibitory interneuron targets.

### Pharmacological identification of P2X<sub>7</sub>Rs in the hippocampus

The pharmacological profile of the receptor mediating the effect of ATP to induce  $[^3H]GABA$  outflow resembles the P2X<sub>7</sub>R phenotype (North and Surprenant 2000; Khakh *et al.* 2001), because:

(i) ATP and BzATP are agonists at this receptor, BzATP being more potent than ATP. As BzATP is not a selective agonist for P2X<sub>7</sub>R, and can bind to other P2X receptors, in particular P2X<sub>1</sub>, P2X<sub>2</sub> and P2X<sub>3</sub> (Bianchi *et al.* 1999), the possibility that other P2X receptors also contributed to the facilitation of GABA release cannot be entirely ruled out. However, it is only at the P2X<sub>7</sub>R that BzATP is more potent than ATP (Bianchi *et al.* 1999), showing the dominant involvement of the P2X<sub>7</sub>R-subtype in this effect. Consequently, the present study focused on the pharmacological and immunohistochemical demonstration of P2X<sub>7</sub>R in the hippocampus whereas identification of other P2X subtypes awaits further investigation.

(ii) The potency of ATP and BzATP were at least one order of magnitude lower than activation of non-P2X<sub>7</sub> P2X receptors and were in millimolar range, consistent with P2X<sub>7</sub>R-mediated responses (e.g. Grahames *et al.* 1999). On the other hand, the short *in situ* half-life (< 200 ms (Cunha *et al.* 1998) and the highly effective degradation of ATP in the hippocampal slice (Dunwiddie *et al.* 1997), offers an explanation why the effective concentrations of ATP were higher in this study than the affinity reported for recombinant P2X<sub>7</sub>R in cellular systems (Khakh *et al.* 2001), where receptor distribution, diffusion properties and drug availability is different than in native tissues. In fact, the agonist potency of ATP could be increased more than 30-fold under ecto-nucleotidase inhibition (Fagura *et al.* 2000), and the observation that the IC<sub>50</sub> values of antagonists in this study were well within the range that it is reported for P2X<sub>7</sub>Rs also supports the assumption, that the agonist availability was selectively decreased in our system.

(iii) Removal of Mg<sup>2+</sup> potentiated the ATP response, which may increase the agonist affinity for P2X<sub>7</sub>R (Virginio *et al.* 1997).

(iv) The selective P2X<sub>7</sub> antagonist Brilliant blue G (Jiang *et al.* 2000) antagonized the response to ATP at low concentrations and pretreatment of the irreversible P2X<sub>7</sub>R antagonist oxiATP also inhibited it. The action of all the antagonists seemed to be non-competitive similarly to that observed for heterologously expressed P2X<sub>7</sub>R (Hibell *et al.* 2001).

(v) Zn<sup>2+</sup>, which is discriminative between P2X<sub>7</sub> and other P2X subunits (Virginio *et al.* 1997), attenuated ATP-induced response.

The only finding that does not readily support the participation of P2X<sub>7</sub>R is that suramin, which inhibits P2X<sub>7</sub>R-mediated responses in recombinant systems (Hibell *et al.* 2001), did not diminish ATP (10 mM)-induced [<sup>3</sup>H]GABA outflow in our study. However, suramin has low affinity to P2X<sub>7</sub>R (North and Surprenant 2000) and in other studies it was also ineffective to antagonize P2X<sub>7</sub>R-mediated pore formation (Chessell *et al.* 1997) and plasminogen release (Inoue *et al.* 1998) in microglial cells.

Moreover, suramin has numerous side-effects, not related to purinoceptor antagonism, e.g. powerful inhibition of ecto-ATPase (Ziganshin *et al.* 1995) and other ATP-utilizing enzymes as well as glutamate and GABA receptors (Motin and Bennett 1995; Nakazawa *et al.* 1995), which could also counterbalance its inhibitory effect on P2X<sub>7</sub>Rs.

A substantial part of the ATP (10 mM)-induced response remained unaffected after the blockade of P2 purinoceptors, by either PPADS or Brilliant blue G, or Zn<sup>2+</sup>. This residual response might be either mediated by PPADS and suramin-insensitive purinoceptors such as the homomeric P2X<sub>4</sub> (North and Surprenant 2000), which is present in the hippocampus (Norenberg and Illes 2000) or due to non-specific effects of ATP, which are unavoidable at this concentration. In fact, an identical change in the Ca<sup>2+</sup> concentration of the medium that caused by ATP (10 mM) elicited alone a small, but detectable release of tritium which could be responsible for as much as 16.4% of the residual release.

#### Expression pattern of the P2X<sub>7</sub> receptor

*In situ* hybridization revealed that mRNA encoding the P2X<sub>7</sub>R was present in neurones in the cell body layers of the hippocampus. However, immunostaining indicated that the cell body layers were almost devoid of labelling, yet the axonal projection fields were strongly stained with punctate reaction product. Electron microscopy revealed that this labelling was due to presynaptic localization of the P2X<sub>7</sub>R. Because the P2X<sub>7</sub>R-immunoreactive pre-synaptic terminals were of the asymmetric type (Gray's type I), were located in the projection fields of the hippocampal principal cells and were not parvalbumin-immunoreactive, we conclude that they are excitatory synapses. Even though mRNA is present in the somatic cytoplasm of the principal neurones the receptor protein is not inserted into the membrane in the somata or dendrites. In contrast, in the terminals we observed labelling adjacent to the membrane, consistent with insertion of the receptor in the membrane since the antibody recognises an intracellular portion of the receptor (see Fig. 6). In addition, reaction product was present in the cytoplasm of the neurones, concordant with trafficking of the receptor to its final site or internalisation upon agonist stimulation as observed in neurones transfected with GFP-tagged P2X<sub>1</sub>R (Li *et al.* 2000).

#### Origin and subcellular mechanism underlying P2X<sub>7</sub>R-induced GABA release

The question arises how P2X<sub>7</sub>R activation on excitatory terminals could influence GABA efflux in the hippocampus (see Fig. 10). As the uptake of tritium into glial cells was prevented by β-alanine, the glial GABA uptake blocker (Iversen and Kelly 1975), one can assume that [<sup>3</sup>H]GABA outflow represents predominantly neuronal GABA release. Because P2 agonists, at least in low concentration, do not

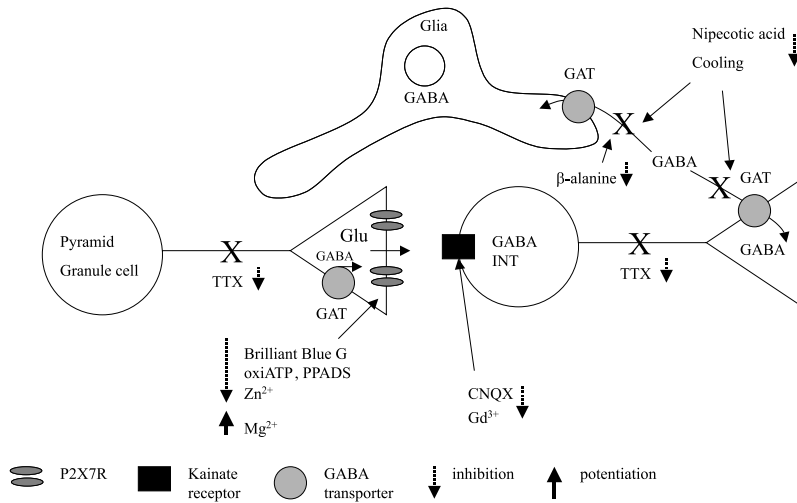


**Fig. 10** Schematic drawing of the concept of how P2X<sub>7</sub>R activation affects neurotransmitter release in the hippocampus. P2X<sub>7</sub>R are highly associated to excitatory nerve terminals in all three regions of the hippocampus and their activation releases GABA and glutamate. The uptake of tritiated GABA into glial cells was prevented during the loading period. As P2X<sub>7</sub>R-induced GABA efflux was partly inhibited by CNQX and Gd<sup>3+</sup>, the origin of GABA seems to be the interneuron

targets of excitatory nerve terminals and the mossy fibre terminals, which also take up and synthesize GABA. Blockade of action potential propagation by TTX prevents GABA efflux from both sources. Cooling the bath temperature and nipepicotic acid also inhibited P2X<sub>7</sub>R-induced GABA efflux, therefore its underlying mechanism seems to be the reversal of the sodium-dependent GABA transporter. Glu, Glutamate, GAT, GABA transporter, INT, interneuron.

promote release of GABA from hippocampal synaptosomal preparations (Cunha and Ribeiro 2000), but ATP releases glutamate in hippocampal neurones in culture (Inoue *et al.* 1992) and in dorsal root ganglion neurones (Gu and MacDermott 1997; Nakatsuka and Gu 2001), it seemed likely that an intact network is necessary for P2X<sub>7</sub>R-evoked GABA release. The predominant synaptic target of excitatory nerve terminals in the CA3 regions are interneurons (Acsady *et al.* 1998), and P2X<sub>7</sub>R immunoreactivity was found in excitatory terminals synapsing onto parvalbumin containing GABAergic target neurones, therefore the most likely source of P2X<sub>7</sub>R-mediated [<sup>3</sup>H]GABA efflux appear these GABAergic target cells. Supporting this hypothesis, TTX (1 µM) and CNQX (10–100 µM) reduced the effect of ATP up to 66% (Fig. 7b), indicating that kainate receptor-mediated transmission is partly involved in this action. This would be consistent with the presence of kainate receptors on hippocampal inhibitory interneurons that can be activated by synaptic stimulation (Frerking *et al.* 1998), the expression of GluR5 and GluR6 by hippocampal interneurons (Paternain *et al.* 2000) and their sensitivity to higher concentrations of CNQX (Castillo *et al.* 1997). In line with this assumption, Gd<sup>3+</sup>, the selective kainate receptor antagonist (Huettnner *et al.* 1998) decreased ATP-induced [<sup>3</sup>H]GABA efflux, whereas GYKI53655, the selective AMPA antagonist (Vignes and Collingridge 1997) was without significant effect. Moreover, ATP and BzATP were also able to release [<sup>14</sup>C]glutamate with a lower potency than that which elicited [<sup>3</sup>H]GABA efflux under an identical application protocol

(Fig. 7b), and BzATP was more potent than ATP, consistent with P2X<sub>7</sub>R activation. This finding is in agreement with recent findings of Krugel *et al.* (2001) who found that ATP stimulates glutamate and subsequent GABA release from the rat nucleus accumbens *in vivo*. It should be noted, however, that apart from [<sup>3</sup>H]GABA efflux, which represents predominantly neuronal GABA release, [<sup>14</sup>C]glutamate efflux could be equally derived from neuronal and non-neuronal cells, e.g. from astrocytes which also express P2X<sub>7</sub>R (John *et al.* 2001) and release glutamate in response to ATP application (Jeremic *et al.* 2001).

A substantial part of ATP-induced [<sup>3</sup>H]GABA efflux remained unaffected after the blockade of the kainate-mediated transmission. Therefore, a potential source of the CNQX-resistant part of P2X<sub>7</sub>R-activated GABA efflux might be the mossy fibre terminals themselves (Fig. 10) or P2X<sub>7</sub>R-expressing astrocytes. Mossy fibre terminals take up and synthesize GABA (Sandler and Smith 1991), which contributes to fast inhibitory GABAergic transmission at the mossy fibre synapse between dentate granule cells and CA1 pyramidal cells (Walker *et al.* 2001). As GABA does not accumulate in the synaptic vesicles (Chaudhry *et al.* 1998) in the mossy fibres, it should leave the terminals in a non-exocytotic, carrier-mediated way. This is convergent with our observation, because blockade of membrane transporters by low temperature, or by the GABA transporter inhibitor nipepicotic acid as well as the inhibition of the sodium influx by TTX all prevented P2X<sub>7</sub>R-induced [<sup>3</sup>H]GABA outflow. Although low temperature might also interfere with P2X<sub>7</sub>R

function, the selective effect of nipecotic acid on ATP-induced [<sup>3</sup>H]GABA release is strongly indicative for the involvement of the GABA carrier in this effect. It is well known that sodium accumulation due to even mild depolarization may reverse the direction of GABA transporters and produce GABA liberation (Köfalvi *et al.* 2000; Wu *et al.* 2001). Therefore, the underlying mechanism of ATP-induced [<sup>3</sup>H]GABA release could be the sodium-dependent reversal of the GABA transporter, present on the terminals of either GABAergic interneurons, or mossy fibres or on astrocytes. In contrast, increased [<sup>3</sup>H]GABA outflow in response to P2X<sub>7</sub>R activation cannot be explained by a reduced uptake by the GABA transporter, because tritium efflux should be increased then by cooling or nipecotic acid.

It is known that long-lasting exposure of agonists at P2X<sub>7</sub>R and other P2X receptors elicit progressive dilatation of the receptor ion channel complex, permitting passage of large molecular weight cations up to 600 kDa (Virginio *et al.* 1997, 1999; Khakh and Lester 1999). To test whether pore dilatation contributes to GABA-releasing effect of ATP, calmidazolium was used, which blocks P2X<sub>7</sub>R-induced ionic currents but not pore formation in HEK293 cells expressing the P2X<sub>7</sub>R (Virginio *et al.* 1997). Calmidazolium reduced approximately 40% of ATP-induced [<sup>3</sup>H]GABA efflux, showing that direct cation influx through the ion channel plays a role in this process but pore formation might be also involved.

#### The role of P2X<sub>7</sub>R activation by endogenous ATP in the modulation of hippocampal synaptic transmission

The presynaptic nerve terminal is a major regulatory site for activity-dependent changes in synaptic function. In our experiments, when hippocampal slices were stimulated by high frequency EFS, which elicited a TTX-sensitive [<sup>3</sup>H]GABA outflow mimicking GABA release by physiological neuronal activity, Brilliant blue G and PPADS significantly decreased EFS-evoked [<sup>3</sup>H]GABA outflow indicating the action of endogenous ATP on P2X<sub>7</sub>Rs. Although PPADS might have other molecular targets than P2X<sub>7</sub>Rs (Ralevic and Burnstock 1998), its effect was prevented by low temperature, the same manipulation that reversed P2X<sub>7</sub>R-activated [<sup>3</sup>H]GABA outflow. These findings indicate that the P2X<sub>7</sub>R is activated by endogenous ATP released during neuronal activity and is likely to play an important role in modulating synaptic transmission. In accordance with our results, PPADS prevented glutamatergic EPSC in synapses between the mossy fibre–CA3 pyramidal cell, and Schaffer collateral–CA1 pyramidal cells (Motin and Bennett 1995). Because ATP release from hippocampal slices is highly frequency-dependent (Wieraszko *et al.* 1989; Cunha *et al.* 1996), and P2X<sub>7</sub>Rs require high concentrations of ATP to be activated (North and Surprenant 2000), it might also serve as an important molecular sensor of increased neuronal activity and contribute to long-term plasticity phenomena, underlying memory formation.

The free ATP concentration present in the cytoplasm is in millimolar range (Gribble *et al.* 2000), therefore an important source of extracellular ATP accumulation might be cellular damage which provides an ATP-rich local milieu nearby the receptors. ATP is released from the brain by energy deprivation (Lutz and Kabler 1997; Jurányi *et al.* 1999) and the up-regulation of ectoATPase enzyme (Braun *et al.* 1998) as well as an intensive expression of P2X<sub>7</sub>R-immunoreactivity (Collo *et al.* 1997) were observed after transient ischaemia which indicates elevated extracellular ATP levels and the pathological activation of P2X<sub>7</sub>Rs under these conditions. Dysregulation of transmitter release is an important factor in ischemia-induced neurodegeneration, and the activation of P2X<sub>7</sub>R may play a critical role in excitotoxicity by increasing release of glutamate from excitatory presynaptic terminals in response to cellular damage. Because P2X<sub>7</sub>Rs are also involved in a number of other processes affecting neuronal survival, e.g. in microglial (Di Virgilio *et al.* 1999) and astroglial activation (John *et al.* 2001; Panenka *et al.* 2001) cytotoxicity (Ferrari *et al.* 1997), the secretion of nitric oxide (Sperlágh *et al.* 1998) and cytokines (Hide *et al.* 2000; Sanz and Di Virgilio 2000), P2X<sub>7</sub>Rs could be a new, intriguing target in neurodegenerative diseases.

#### Acknowledgements

This study was supported by the grants of the Hungarian Research Foundation (OTKA T025614, T037457), Hungarian Medical Research Council (ETT27/2000), The Wellcome Trust, The Volkswagen Foundation and by the Centre of Excellence grant of EU Framework Program 5 (ICA1-CT-2000-70004). The authors are grateful for Mária Baranyi for HPLC analysis and István Tarnawa for donation of GYKI 53655.

#### References

- Acsady L., Kamondi A., Sik A., Freund T. and Buzsáki G. (1998) GABAergic cells are the major postsynaptic targets of mossy fibers in the rat hippocampus. *J. Neurosci.* **18**, 3386–3403.
- Atkinson L., Batten T. F. C. and Deuchars J. (2000) P2X<sub>2</sub> receptor immunoreactivity in the dorsal vagal complex and area postrema of the rat. *Neuroscience* **99**, 683–696.
- Bahena-Trujillo R. and Arias-Montano J. A. (1999) [<sup>3</sup>H]gamma-aminobutyric acid transport in rat substantia nigra pars reticulata synaptosomes: pharmacological characterization and phorbol ester-induced inhibition. *Neurosci. Lett.* **274**, 119–122.
- Bianchi B. R., Lynch K. J., Touma E., Niforatos W., Burgard E. C., Alexander K. M., Park H. S., Yu H., Metzger R., Kowaluk E., Jarvis M. F. and van Biesen T. (1999) Pharmacological characterization of recombinant human and rat P2X receptor subtypes. *Eur. J. Pharmacol.* **376**, 127–138.
- Brandle U., Kohler K. and Wheeler-Schilling T. H. (1998) Expression of the P2X<sub>7</sub>-receptor subunit in neurons of the rat retina. *Brain Res. Mol. Brain Res.* **62**, 106–109.
- Brandle U., Zenner H. P. and Ruppersberg J. P. (1999) Gene expression of P2X-receptors in the developing inner ear of the rat. *Neurosci. Lett.* **273**, 105–108.

- Braun N., Zhu Y., Krieglstein J., Culmsee C. and Zimmermann H. (1998) Upregulation of the enzyme chain hydrolyzing extracellular ATP after transient forebrain ischemia in the rat. *J. Neurosci.* **18**, 4891–4900.
- Burnstock G. (1999) Current status of purinergic signalling in the nervous system. *Prog. Brain Res.* **120**, 3–10.
- Castillo P. E., Malenka R. C. and Nicoll R. A. (1997) Kainate receptors mediate a slow postsynaptic current in hippocampal CA3 neurons. *Nature* **388**, 182–186.
- Chaudhry F. A., Reimer R. J., Bellocchio E. E., Danbolt N. C., Osen K. K., Edwards R. H. and Storm-Mathisen J. (1998) The vesicular GABA transporter, VGAT, localizes to synaptic vesicles in sets of glycinergic as well as GABAergic neurons. *J. Neurosci.* **18**, 9733–9750.
- Chessell I. P., Michel A. D. and Humphrey P. P. (1997) Properties of the pore-forming P2X<sub>7</sub> purinoceptor in mouse NTW8 microglial cells. *Br. J. Pharmacol.* **121**, 1429–1437.
- Collo G., Neidhart S., Kawashima E., Kosco-Vilbois M., North R. A. and Buell G. (1997) Tissue distribution of the P2X<sub>7</sub> receptor. *Neuropharmacology* **36**, 1277–1283.
- Cunha R. A. and Ribeiro J. A. (2000) Purinergic modulation of [<sup>3</sup>H]GABA release from rat hippocampal nerve terminals. *Neuropharmacology* **39**, 1156–1167.
- Cunha R. A., Sebastiao A. M. and Ribeiro J. A. (1998) Inhibition by ATP of hippocampal synaptic transmission requires localized extracellular catabolism by ecto-nucleotidases into adenosine and channeling to adenosine A1 receptors. *J. Neurosci.* **18**, 1987–1995.
- Cunha R. A., Vizi E. S., Ribeiro J. A. and Sebastiao A. M. (1996) Preferential release of ATP and its extracellular catabolism as a source of adenosine upon high- but not low-frequency stimulation of rat hippocampal slices. *J. Neurochem.* **67**, 2180–2187.
- Deuchars S. A., Atkinson L., Brooke R. E., Musa H., Milligan C. J., Batten T. F. C., Buckley N. J., Parson S. H. and Deuchars J. (2001) Neuronal P2X<sub>7</sub> receptors are targeted to presynaptic terminals in the central and peripheral nervous systems. *J. Neurosci.* **21**, 7143–7152.
- Di Iorio P., Battaglia G., Ciccarelli R., Ballerini P., Giuliani P., Poli A., Nicoletti F. and Caciagli F. (1996) Interaction between A1 adenosine and class II metabotropic glutamate receptors in the regulation of purine and glutamate release from rat hippocampal slices. *J. Neurochem.* **67**, 302–309.
- Di Virgilio F., Sanz J. M., Chiozzi P. and Falzoni S. (1999) The P2Z/P2X<sub>7</sub> receptor of microglial cells: a novel immunomodulatory receptor. *Prog. Brain Res.* **120**, 355–368.
- Dunwiddie T. V., Diao L. and Proctor W. R. (1997) Adenine nucleotides undergo rapid, quantitative conversion to adenosine in the extracellular space in rat hippocampus. *J. Neurosci.* **17**, 7673–7682.
- Edwards F. A., Gibb A. J. and Colquhoun D. (1992) ATP receptor-mediated synaptic currents in the central nervous system. *Nature* **359**, 144–147.
- Figura M. S., Jarvis G. E., Dougall I. G. and Leff P. (2000) Adventures in the pharmacological analysis of P2 receptors. *J. Auton. Nerv. Syst.* **81**, 178–186.
- Ferrari D., Chiozzi P., Falzoni S., Dal Susino M., Collo G., Buell G. and Di Virgilio F. (1997) ATP-mediated cytotoxicity in microglial cells. *Neuropharmacology* **36**, 1295–1301.
- Frerking M., Malenka R. C. and Nicoll R. A. (1998) Synaptic activation of kainate receptors on hippocampal interneurons. *Nat. Neurosci.* **1**, 479–486.
- Grahames C. B., Michel A. D., Chessell I. P. and Humphrey P. P. (1999) Pharmacological characterization of ATP- and LPS-induced IL-1 $\beta$  release in human monocytes. *Br. J. Pharmacol.* **127**, 1915–1921.
- Gribble F. M. L. G., Tucker S. J., Zhao C., Nichols C. G. and Ashcroft F. M. (2000) A new method for measurement of sub-membrane ATP concentration. *J. Biol. Chem.* **275**, 30046–30049.
- Gu J. G. and MacDermott A. B. (1997) Activation of ATP P2X receptors elicits glutamate release from sensory neuron synapses. *Nature* **389**, 749–753.
- Hibell A. D., Thompson K. M., Xing M., Humphrey P. P. and Michel A. D. (2001) Complexities of measuring antagonist potency at P2X<sub>7</sub> receptor orthologues. *J. Pharmacol. Exp. Ther.* **296**, 947–957.
- Hide I., Tanaka M., Inoue A., Nakajima K., Kohsaka S., Inoue K. and Nakata Y. (2000) Extracellular ATP triggers tumor necrosis factor- $\alpha$  release from rat microglia. *J. Neurochem.* **75**, 965–972.
- Huettner J. E., Stack E. and Wilding T. J. (1998) Antagonism of neuronal kainate receptors by lanthanum and gadolinium. *Neuropharmacology* **37**, 1239–1247.
- Hugel S. and Schlichter R. (2000) Presynaptic P2X receptors facilitate inhibitory GABAergic transmission between cultured rat spinal cord dorsal horn neurons. *J. Neurosci.* **20**, 2121–2130.
- Illes P., Klotz K.-N. and Lohse M. J. (2000) Signaling by extracellular nucleotides and nucleosides. *Naunyn Schmiedeberg's Arch. Pharmacol.* **362**, 295–299.
- Inoue K., Nakajima K., Morimoto T., Kikuchi Y., Koizumi S., Illes P. and Kohsaka S. (1998) ATP stimulation of Ca<sup>2+</sup>-dependent plasminogen release from cultured microglia. *Br. J. Pharmacol.* **123**, 1304–1310.
- Inoue K., Nakazawa K., Fujimori K., Watano T. and Takanaka A. (1992) Extracellular adenosine 5'-triphosphate-evoked glutamate release in cultured hippocampal neurons. *Neurosci. Lett.* **134**, 215–218.
- Iversen L. L. and Kelly J. S. (1975) Uptake and metabolism of gamma-aminobutyric acid by neurones and glial cells. *Biochem. Pharmacol.* **24**, 933–938.
- Jeremic A., Jefinija K., Stevanovic J., Glavaski A. and Jefinija S. (2001) ATP stimulates calcium-dependent glutamate release from cultured astrocytes. *J. Neurochem.* **77**, 664–675.
- Jiang L. H., Mackenzie A. B., North R. A. and Surprenant A. (2000) Brilliant blue G selectively blocks ATP-gated rat P2X<sub>7</sub> receptors. *Mol. Pharmacol.* **58**, 82–88.
- John G. R., Simpson J. E., Woodroffe M. N., Lee S. C. and Brosnan C. F. (2001) Extracellular nucleotides differentially regulate interleukin-1 $\beta$  signaling in primary human astrocytes: implications for inflammatory gene expression. *J. Neurosci.* **21**, 4134–4142.
- Jurányi Z., Sperlágh B. and Vizi E. S. (1999) Involvement of P2 purinoceptors and the nitric oxide pathway in [<sup>3</sup>H]purine outflow evoked by short-term hypoxia and hypoglycemia in rat hippocampal slices. *Brain Res.* **823**, 183–190.
- Katona I., Sperlágh B., Sik A., Kofalvi A., Vizi E. S., Mackie K. and Freund T. F. (1999) Presynaptically located CB1 cannabinoid receptors regulate GABA release from axon terminals of specific hippocampal interneurons. *J. Neurosci.* **19**, 4544–4558.
- Kennedy C. and Leff P. (1995) How should P2X purinoceptors be classified pharmacologically? *Trends Pharmacol. Sci.* **16**, 168–174.
- Khakh B. S. (2001) Molecular physiology of P2X receptors and ATP signalling at synapses. *Nat. Rev.* **2**, 165–174.
- Khakh B. S., Burnstock G., Kennedy C., King B. F., North A., Séguela P., Voigt M. and Humphrey P. A. (2001) International Union of Pharmacology. XXIV: Current status of the nomenclature and properties of P2X receptors and their subunits. *Pharmacol. Rev.* **53**, 107–118.
- Khakh B. S. and Lester H. A. (1999) Dynamic selectivity filters in ion channels. *Neuron* **23**, 653–658.
- Kim M., Spelta V., Sim J., North R. A. and Surprenant A. (2001) Differential assembly of rat purinergic P2X<sub>7</sub> receptor in immune cells of the brain and periphery. *J. Biol. Chem.* **276**, 23262–23267.
- Kofalvi A., Sperlágh B., Zelles T. and Vizi E. S. (2000) Long-lasting facilitation of 4-amino-n-[2,3-<sup>3</sup>H]butyric acid ([<sup>3</sup>H]GABA) release

- from rat hippocampal slices by nicotinic receptor activation. *J. Pharmacol. Exp. Ther.* **295**, 453–462.
- Krogsgaard-Larsen P. and Johnston G. A. (1975) Inhibition of GABA uptake in rat brain slices by nipecotic acid, various isoxazoles and related compounds. *J. Neurochem.* **25**, 797–802.
- Krugel U., Kittner H. and Illes P. (2001) Mechanisms of adenosine 5'-triphosphate-induced dopamine release in the rat nucleus accumbens *in vivo*. *Synapse* **39**, 222–232.
- Li G. H., Lee E. M., Blair D., Holding C., Poronnik P., Cook D. I., Barden J. A. and Bennett M. R. (2000) The distribution of P2X receptor clusters on individual neurons in sympathetic ganglia and their redistribution on agonist activation. *J. Biol. Chem.* **275**, 29107–29112.
- Lutz P. L. and Kabler S. (1997) Release of adenosine and ATP in the brain of the freshwater turtle (*Trachemys scripta*) during long-term anoxia. *Brain Res.* **769**, 281–286.
- Milusheva E., Baranyi M., Zelles T., Mike A. and Vizi E. S. (1994) Release of acetylcholine and noradrenaline from the cholinergic and adrenergic afferents in rat hippocampal CA1, CA3 and dentate gyrus regions. *Eur. J. Neurosci.* **6**, 187–192.
- Mori M., Heuss C., Gahwiler B. H. and Gerber U. (2001) Fast synaptic transmission mediated by P2X receptors in CA3 pyramidal cells of rat hippocampal slice cultures. *J. Physiol.* **535**, 115–123.
- Motin L. and Bennett M. R. (1995) Effect of P2-purinoreceptor antagonists on glutamatergic transmission in the rat hippocampus. *Br. J. Pharmacol.* **115**, 1276–1280.
- Nakai T., Milusheva E., Baranyi M., Uchihashi Y., Satoh T. and Vizi E. S. (1999) Excessive release of [<sup>3</sup>H]noradrenaline and glutamate in response to simulation of ischemic conditions in rat spinal cord slice preparation: effect of NMDA and AMPA receptor antagonists. *Eur. J. Pharmacol.* **366**, 143–150.
- Nakatsuka T. and Gu J. G. (2001) ATP P2X receptor-mediated enhancement of glutamate release and evoked EPSCs in dorsal horn neurons of the rat spinal cord. *J. Neurosci.* **21**, 6522–6531.
- Nakazawa K., Inoue K., Ito K. and Koizumi S. (1995) Inhibition by suramin and reactive blue 2 of GABA and glutamate receptor channels in rat hippocampal neurons. *Naunyn Schmiedeberg's Arch. Pharmacol.* **351**, 202–208.
- Norenberg W. and Illes P. (2000) Neuronal P2X receptors: localization and functional properties. *Naunyn Schmiedeberg's Arch. Pharmacol.* **362**, 324–340.
- North R. A. and Surprenant A. (2000) Pharmacology of cloned P2X receptors. *Annu. Rev. Pharmacol. Toxicol.* **40**, 563–580.
- Panenka W., Jijon H., Herx L. M., Armstrong J. N., Feighan D., Wei T., Yong V. W., Ransohoff R. M. and MacVicar B. A. (2001) P2X<sub>7</sub>-like receptor activation in astrocytes increases chemokine monocyte chemoattractant protein-1 expression via mitogen-activated protein kinase. *J. Neurosci.* **21**, 7135–7142.
- Pankratov Y., Castro E., Miras-Portugal M. T. and Krishtal O. (1998) A purinergic component of the excitatory postsynaptic current mediated by P2X receptors in the CA1 neurons of the rat hippocampus. *Eur. J. Neurosci.* **10**, 3898–3902.
- Paternain A. V., Herrera M. T., Nieto M. A. and Lerma J. (2000) GluR5 and GluR6 kainate receptor subunits coexist in hippocampal neurons and co-assemble to form functional receptors. *J. Neurosci.* **20**, 196–205.
- Ralevic V. and Burnstock G. (1998) Receptors for purines and pyrimidines. *Pharmacol. Rev.* **50**, 413–492.
- Rubio M. and Soto F. (2001) Distinct localization of P2X receptors at excitatory post-synaptic specializations. *J. Neurosci.* **21**, 641–653.
- Sandler R. and Smith A. D. (1991) Coexistence of GABA and glutamate in mossy fiber terminals of the primate hippocampus: an ultrastructural study. *J. Comp. Neurol.* **303**, 177–192.
- Sanz J. M. and Di Virgilio F. (2000) Kinetics and mechanism of ATP-dependent IL-1 beta release from microglial cells. *J. Immunol.* **164**, 4893–4898.
- Sperlágh B. and Vizi E. S. (1991) Effect of presynaptic P2 receptor stimulation on transmitter release. *J. Neurochem.* **56**, 1466–1470.
- Sperlágh B. and Vizi E. S. (1996) Neuronal synthesis, storage and release of ATP. *Semin. Neurosci.* **8**, 175–186.
- Sperlágh B., Erdelyi F., Szabo G. and Vizi E. S. (2000) Local regulation of [(3) H]-noradrenaline release from the isolated guinea-pig right atrium by P<sub>2X</sub>-receptors located on axon terminals. *Br. J. Pharmacol.* **131**, 1775–1783.
- Sperlágh B., Hasko G., Nemeth Z. and Vizi E. S. (1998) ATP released by LPS increases nitric oxide production in RAW 264.7 macrophage cell line via P2Z/P2X<sub>7</sub> receptors. *Neurochem. Int.* **33**, 209–215.
- Sperlágh B. and Vizi E. S. (2000) Regulation of purine release, in Purinergic and Pyrimidinergic Signalling I. In: *Molecular, Nervous and Urogenital System Function*, Vol. 151/1 (Abbracchio M. P. & Williams M., eds), pp. 179–208. Springer, Berlin.
- Surprenant A., Rassendren F., Kawashima E., North R. A. and Buell G. (1996) The cytolytic P2Z receptor for extracellular ATP identified as a P2X receptor (P2X<sub>7</sub>). *Science* **272**, 735–738.
- Torres G. E., Egan T. M. and Voigt M. M. (1999) Hetero-oligomeric assembly of P2X receptor subunits. Specificities exist with regard to possible partners. *J. Biol. Chem.* **274**, 6653–6659.
- Vignes M. and Collingridge G. L. (1997) The synaptic activation of kainate receptors. *Nature* **388**, 179–182.
- Virginio C., Church D., North R. A. and Surprenant A. (1997) Effects of divalent cations, protons and calmidazolium at the rat P2X<sub>7</sub> receptor. *Neuropharmacology* **36**, 1285–1294.
- Virginio C., MacKenzie A., North R. A. and Surprenant A. (1999) Kinetics of cell lysis, dye uptake and permeability changes in cells expressing the rat P2X<sub>7</sub> receptor. *J. Physiol.* **519**, 335–346.
- Visentin S., Renzi M., Frank C., Greco A. and Levi G. (1999) Two different ionotropic receptors are activated by ATP in rat microglia. *J. Physiol.* **519**, 723–736.
- Vizi E. S. (1998) Different temperature dependence of carrier-mediated (cytoplasmic) and stimulus-evoked (exocytotic) release of transmitter: a simple method to separate the two types of release. *Neurochem. Int.* **33**, 359–366.
- Vizi E. S. and Sperlágh B. (1999) Separation of carrier mediated and vesicular release of GABA from rat brain slices. *Neurochem. Int.* **34**, 407–413.
- Walker M. C., Ruiz A. and Kullmann D. M. (2001) Monosynaptic GABAergic signaling from dentate to CA3 with a pharmacological and physiological profile typical of mossy fiber synapses. *Neuron* **29**, 703–715.
- Wieraszko A., Goldsmith G. and Seyfried T. N. (1989) Stimulation-dependent release of adenosine triphosphate from hippocampal slices. *Brain Res.* **485**, 244–250.
- Wu Y., Wang W. and Richerson G. B. (2001) GABA transaminase inhibition induces spontaneous and enhances depolarization-evoked GABA efflux via reversal of the GABA transporter. *J. Neurosci.* **21**, 2630–2639.
- Ziganshin A. U., Ziganshina L. E., King B. E. and Burnstock G. (1995) Characteristics of ecto-ATPase of *Xenopus* oocytes and the inhibitory actions of suramin on ATP breakdown. *Pflugers Arch.* **429**, 12–418.